

RICOCHET OF SPINNING SPHERES OFF WATER

RIYAH NAJIM KITER¹, MAZIN YASEEN ABBOOD¹ AND OMAR HASHIM HASSOON^{2*}

¹Department of Mechanical Engineering, College of Engineering, University of Anbar, Iraq

²Department of Production Engineering and Metallurgy, University of Technology, Baghdad, Iraq

*Corresponding author: omar.h.hassoon@uotechnology.edu.iq

(Received: 17th May 2022; Accepted: 5th October 2022; Published on-line: 4th January 2023)

ABSTRACT: Liquid impact and ricochet is still attracting researchers interested in the field of hydrodynamics and naval engineering. The ricochet from a water surface experienced by spinning spheres was examined both analytically and numerically. A theoretical analysis was made to quantify the enhancement attained by imparting backspin to the sphere. Numerical simulation of the process was conducted by implementing ABAQUS software. The mathematical analysis and the simulation were built on the assumption that the effects of cavitation, splash, and two phase flow are negligible compared to hydro-dynamical forces of lift and drag. It was proven that both mathematical analysis and simulation were capable of predicting the trajectory of a spinning sphere during its course of entry into the water. Aspects like the critical angle of ricochet and the maximum depth of immersion were extracted from these trajectories and compared with available data. It was found that the analytical and numerical results were generally validated with respect to each other as well as to existing findings. Aluminum ($\sigma = 2.7$) spinning spheres, of radius 10 mm and speed of 10 m/sec, were examined. It was found that a 300 rad/sec backspin improves the critical angle of ricochet from 10.43 to 12.5 deg and increases the maximum depth of immersion from 1.52 to 1.83. "Magnus Effect" usually acting on a fully immersed spinning sphere, was described and relations estimating the hydrodynamic forces were deduced.

ABSTRAK: Keadaan pertumbuhan bakteri penghasil enzim protease aktif-sejuk terasing daripada sampel Antartika disaring menggunakan satu-faktor-satu-masa (OFAT). Kemudian, enzim protease ini diekstrak pada lewat fasa logaritma untuk ujian enzimatik. Strain yang menunjukkan aktiviti enzim tertinggi telah dipilih bagi tujuan pengoptimuman melalui Kaedah Permukaan Tindak Balas (RSM). Parameter yang dikaji adalah pada suhu pengeraman (4 - 36 °C), media pH (4 - 10) dan kepekatan NaCl (0 - 8 %). Berdasarkan dapatan OFAT, kesemua lapan bakteria menunjukkan kadar pertumbuhan tertinggi pada 20 °C, pH 7 dan 4% NaCl (w/v). Hasil ujian enzimatik menunjukkan enzim protease mentah yang diekstrak daripada SC8 menunjukkan aktiviti yang jauh lebih tinggi (0.20 U dan 0.37 U) daripada kawalan positif (0.11 U dan 0.31 U) pada -20 °C dan 20 °C. RSM ini menunjukkan kadar optimum bagi pertumbuhan SC8 adalah pada 20.5 °C, pH 6.83 dan 2.05% NaCl (w/v) dengan dapatan kadar pertumbuhan bakteria pada $3.70 \pm 0.06 \times 10^6$ sel/jam. Keadaan pertumbuhan optimum SC8 melalui kajian ini bermanfaat bagi menghasilkan produk protease aktif-sejuk secara besar-besaran pada masa hadapan.

KEYWORDS: Magnus; water-entry bodies; Ricochet behavior; bouncing rigid body

1. INTRODUCTION

The phenomenon of liquid impact and ricochet is still attracting researchers interested in the field of hydrodynamics and naval engineering. It also fascinates the layman, as evidenced by attempting to achieve skipping of stones across the water's surface. The interaction between liquids and solids in many modern applications has stimulated engineers and scholars to conduct more research towards comprehensive understanding of the phenomenon. These applications include – but are not limited to - ships, offshore structures, missiles, torpedoes, underwater vehicles, watercrafts, and oceanographic measuring devices. Interest in the liquid-solid impact may well stem from the historical technique of ricocheting cannonballs to attack ships in the past two centuries. In this context, the famous bomb used in World War II and known as the Barnes Wallis's bouncing bomb, is particularly recognized. Barnes Wallis proposed an attack on German dams which were protected against normal high-level air attacks. A torpedo attack was also excluded for the defenders of those dams had arranged a web of heavy anti-torpedo netting. He thus proposed spherical bombs dropped from low-level flying aircraft; being too low and too speedy, the bombs would ricochet and skip over the nets. In addition, Wallis succeeded to impart back-spin to the flying bomb for more stability during flight and the ability to ricochet; for more details about this fascinating device, the reader is referred to Johnson [1].

During this period, the water-entry of solid bodies was experimentally investigated by Richardson [2]. A movie camera of 200 frames per second was used to record the trajectories of Duralumin, Steel, and ebonite spheres during their impacts onto water at different combinations of speed and angle, see Fig. 1. Measurements of the entry and exit speeds and angles were also made.

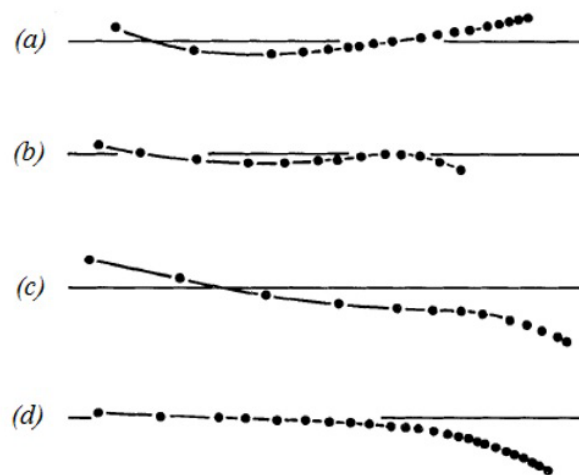


Fig. 1: Depiction of sphere trajectories [2].

It has also been noted that the sphere was always followed by a cavity due to the separation which occurs immediately after contact. In addition, the critical angle of ricochet was found to be 60, 90, and 150 for Steel ($\sigma = 7.8$), Duralumin ($\sigma = 2.7$), and Ebonite ($\sigma = 1.1$), respectively. Finally, the submergence of ricocheting spheres falls in the range of one radius to two.

The first formula appeared in the literature which governs the critical angle of entry of a spherical object for ricochet is due to Birkhoff et al. [3], i.e.:

$$\vartheta_c = \frac{18}{\sqrt{\sigma}} (\text{degrees}) \quad (1)$$

In reproducing Eq. (1), Johnson & Reid [4] adopted the assumptions made in [3] which were: i. the pressure on a surface element is $0.5\rho(V\cos\beta)^2$, ii. the pressure of splash above the undisturbed surface of water is discounted, and iii. the limiting condition for ricochet is that the sphere moves horizontally at the instance of full immersion. No attempt was made to justify these assumptions. Thus, Johnson & Reid [4] concluded that:

$$\vartheta_c = \frac{17.5}{\sqrt{\sigma}} (\text{degrees}) \quad (2)$$

Trajectories for the sphere having different combinations of (V_0, θ_0) were also calculated by applying the equations of motion in both x and y directions.

The effect of spin on the critical angle of ricochet of a cylinder was firstly examined by Hutchings [5]. To this end, and realizing the infeasibility of using the pressure formula $0.5\rho(V\cos\beta)^2$, he adopted the Rayleigh pressure formula, namely:

$$p = \frac{\pi\cos\beta}{4 + \pi\cos\beta} \rho V^2 \quad (3)$$

In addition, Hutchings [5] assumed that: i. the angular extent of the wetted area is twice that used by Johnson & Reid [4] due to splash of water ahead of the sphere, and thus, ii. the limiting condition for ricochet is that the sphere moves horizontally at the instance of the centroid of sphere just reaches the undisturbed surface of water. In this way, Hutchings [5] reported that for a non-spinning sphere:

$$\vartheta_c = \frac{17.3}{\sqrt{\sigma}} (\text{degrees}) \quad (4)$$

So far, the weight of the spherical projectile was assumed negligible in comparison with the hydrodynamic forces at high speeds. At relatively low speeds, however, the effect of projectile weight has to be considered. Following the procedure of Johnson & Reid [4], the weight and hence the speed of sphere has been accounted for by Soliman et al. [6] as:

$$\vartheta_g^2 = \vartheta_c^2 - \frac{4}{\bar{F}} \quad (5)$$

where ϑ_c is that of Eq. (2) and ϑ_g is the new one modified for the speed of sphere. Soliman et al. [6] also carried out tests on the ricochet of Steel and Duralumin spheres from shallow depths of water. Different values of the speed of sphere and the angle of attack were employed. A minimum value of 30 ft/sec was required for Steel spheres in order to achieve ricochet. The effect of spin, albeit uncontrolled, was furthermore explored; only forward spin has been achieved due to which smaller angle was observed for ricochet.

Miloh & Shukron [7] strongly criticized the assumptions made in [3-6], describing it as lack in physical rigor. They formulated the Kelvin-Kirchoff-Lagrange equations of motion based on the energy method assuming large impact velocity. The formulation was performed in terms of time-dependent added-mass coefficients and their time derivatives. No pressure distribution over the sphere surface is prescribed since the method temporarily evaluates the added-mass coefficients and their time-derivatives in the high-frequency limit where the spray energy is ignored with respect to the total kinetic energy of water. Moreover, the

limiting condition for ricochet is that the sphere is just above the undisturbed surface and has zero normal velocity. It was found that the submergence of ricocheting sphere in no time exceeds 1.4 times its radius, even for infinite speed and density of the sphere. Also, the value of critical angle for ricochet predicted by Eq. (1) was found by Miloh & Shukron [7] to represent the infinite Froude number asymptote of their analytic solution. Finally, they predicted a threshold value of Froude number below which a ricochet is not possible, no matter how small the angle. This number is directly proportional with the density of the sphere.

Numerical methods have also been employed for the solution of the ricochet problem, like the source panel method [8] where impact forces and ricochet behavior of the arbitrary-shaped solid bodies can be computed. A disk cylinder and two tangent ogives were tested for validation of the method.

The effect of spin on the characteristics of skipping of thin flat disks was addressed by Rosellini et al. [9]. Experiments revealed a positive effect on the ricochet occurrence through enhancing the aerodynamic stability due to gyroscopic effects. No effect of the spin was noted on the angle of attack. In addition, the number of skips was found to be in direct proportionality with the linear velocity of disk.

An interesting extensive work by Truscot & Techet [10] investigated the effect of spin on the aspects of normal water-entry of a sphere. Controlled spin about the horizontal axis was imparted to standard billiard balls and projected normally onto water surface. Different values of spin and linear speed were attempted to explore their influence on the sphere trajectory and the splash and cavity dynamics. Figure 2 includes images of the cavity and splash as well as the trajectory of non-spinning (left) and spinning (right) spheres.

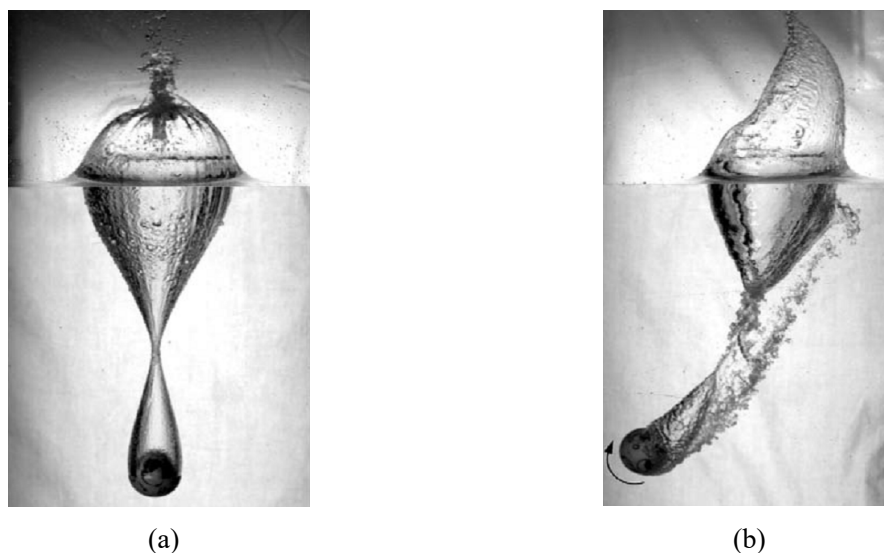


Fig. 2: Images of the cavity and splash as well as the trajectory of 57 mm diameter spheres. (a) non-spinning: $V= 5.95$ m/s. (b) spinning $V=5.45$ m/s, $\text{spin}=251$ rad/s. Both images were taken at the same time after impact ($t=102$ ms). [10]

The apparent curvature in the trajectory of the spinning sphere was attributed to the lift widely known as "Magnus effect"; the lift force increased with spin increase.

The oblique impact of a torpedo onto water was studied theoretically, numerically, and experimentally by Wei et al. [11]. The linear and angular motions of a torpedo were

formulated and solved for the trajectory. MSC DYTRAN was used to simulate the water entry, and the wind tunnel experimentation was based on the similarity principle.

Moxnes et al. [12] used AUTODYN code with the Smooth Particle Hydrodynamics (SPH) method to simulate the ricochet of a spherical steel projectile from the water surface. The simulation with AUTODYN showed too large a drag coefficient but the critical angle of ricochet was consistent with Eq. (1).

Numerical solution of the ricochet of solid non-spinning cylinders from water surface was investigated by Omidvar et al. [13] where fixed ghost boundary conditions were added to Smooth Particle Hydrodynamics (SPH) open source code. It was concluded that the Smoothed Particle Hydrodynamics is a suitable method to investigate the water impact of solid objects.

Recently, Nguyen et al. [14] extended and applied a two-phase three-equation model to simulate the ricochet of circular cylinders from water surface. The numerical method was solved for a cylinder with different densities, and comparisons of predicted and experimental data showed fairly good agreement, which confirmed the capability and robustness of the model for accurate simulation of free surface and water impact flows.

Nguyen et al. [15] presented an efficient free surface solver to simulate the three dimensional modeling of the ricochet problems for solid bodies entries to the water. A dynamic numerical scheme was implemented of grid to facilitate the flow simulation of the complex geometries entered to water.

Lyu et al. [16] experimentally studied the impact of a bouncing sphere to the water surface. The effect of impact velocity and initial impact angle and the energy dissipation on the ricochet of spheres were evaluated. Also the cavitation effect on ricochet were conducted. The study showed that more than half of the initial energy was dissipated at low impact angles.

The authors believe that the ricochet of solids off liquid surfaces is far from exhaustive, particularly in the cases where spinning is involved. In the absence of available theoretical estimate of the critical angle of ricochet associated with spinning spheres, it is hoped that this work will fill some the blanks.

2. THEORETICAL ANALYSIS

Most of the criticisms cited regarding theoretical analyses are focused on the assumptions made prior to, or throughout the analysis, especially those made not on a physical- but on ad hoc- basis. Approximations are another source of precision loss too. In this work, only necessary assumptions, pertaining to the physics of the problem and leading to feasible and reasonable results, will be made. Moreover, the oft-neglected terms (based on their insignificance) will be retained or at least partly sacrificed. The present analysis is based on the following:

1. The hydrodynamic pressure on an elemental surface whose normal makes an angle $\beta \leq \frac{\pi}{2}$ with oncoming stream of non-viscous fluid is that due to Rayleigh - Eq.(3). As stated in the preceding section, Hutchings [5] used this formula in order that the spin effect can be accounted for.

2. The effects of cavitation, splash and two phase flow are negligible compared to the hydro-dynamic forces of lift and drag. Thus, the pressure is primarily due to the equipotential undisturbed surface of the water.

3. The limiting condition for ricochet is that the whole sphere is just above the undisturbed surface and has zero normal velocity.

4. Gravitational forces are introduced in order that the speed and radius of the sphere can be accounted for.

Referring to Fig. 3(A), a backwards spinning sphere enters a calm plane surface of water at an intermediate stage where the sphere has entered a distance y , attained a current speed V in the direction inclined at angle. The wetted portion of the sphere (shown shaded in the figure) extends from $\varphi = 0$, or $y' - axis$ to $\varphi = \varphi_0$.

The hydrodynamic force normal to a surface element of area dS is:

$$dF_n = p dS \tag{6}$$

where, after Hutchings [5]:

$$p = \frac{\pi \cos \beta}{4 + \pi \cos \beta} \rho V'^2 \cong \frac{\pi}{5} \rho V'^2 \cos \beta \tag{7}$$

The elemental area can be calculated as:

$$dS = a^2 \sin \varphi \cdot d\varphi d\psi \tag{8}$$

The resultant velocity V' of a point on the element relative to oncoming water is given by:

$$V'^2 = V^2 + 2r\omega V \cos \alpha + r^2 \omega^2 \tag{9}$$

From Fig. 3(B), it is shown that:

$$r \cos \alpha = a \cos \varphi \tag{10}$$

$$r \sin \alpha = a \sin \varphi \cdot \cos \psi \tag{11}$$

It can easily be shown that:

$$V' \cos \beta = V \sin \varphi \cdot \cos \psi \tag{12}$$

As a result:

$$dF_n = \frac{\pi}{5} \rho V V' a^2 \sin^2 \varphi \cdot \cos \psi \cdot d\varphi d\psi \tag{13}$$

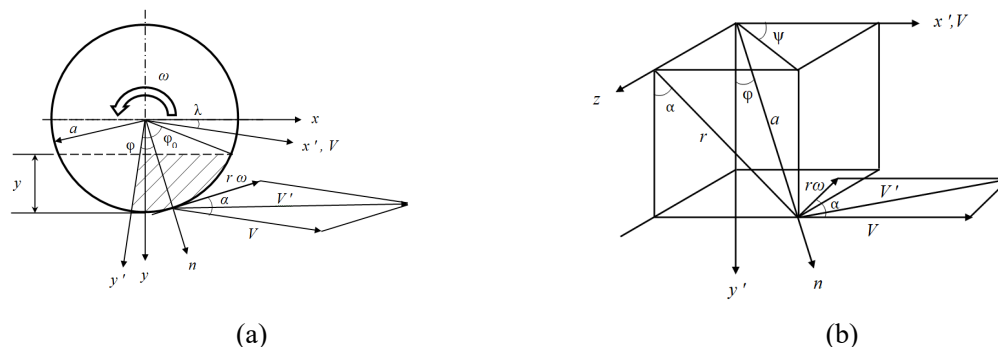


Fig. 3: (a) Velocity vectors on spinning sphere and (b) Relation between the radius of sphere and radius of rotation.

It is noteworthy to distinguish between two intervals in terms of depth of submergence: the first interval, shown in Fig. 4, in which $0 \leq y \leq a(1 - \cos\lambda)$, and the second interval in which $y > a(1 - \cos\lambda)$, see Fig. 3(A). These intervals are differentiated through the parameter, δ , where:

$$\delta = \begin{cases} \lambda - \gamma & , \quad 0 \leq \gamma \leq \lambda \\ 0 & , \quad \gamma > \lambda \end{cases} \quad (14)$$

$$\gamma = \cos^{-1} \frac{a - y}{a} \quad (15)$$

$$\varphi_0 = \lambda + \gamma \quad (16)$$

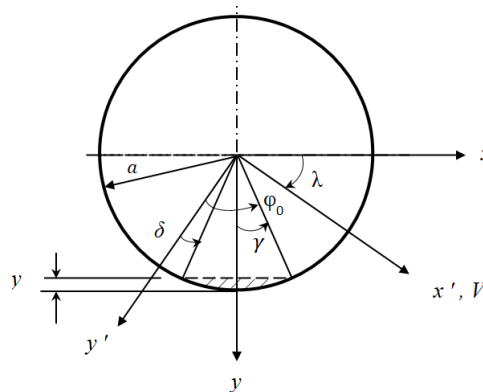


Fig. 4: First stage of wetted portion is shown shaded.

The drag force, D , along x' - axis is given by:

$$D = \int_S^{\varphi_0} dF_n \cdot \sin\varphi \cdot \cos\psi \quad (17)$$

or:

$$D = \frac{\pi}{5} \rho a^2 \int_{\delta}^{\varphi_0} 2 \int_0^{\frac{\pi}{2}} \sqrt{V^2 + 2r\omega V \cos\alpha + r^2\omega^2} \cdot V \sin^3\varphi \cdot \cos^2\psi \cdot d\varphi d\psi \quad (18)$$

The integration is performed over the leading half of the sphere below the undisturbed surface of water. At this stage, one may neglect the $r^2\omega^2$ term and still seek a numerical solution or retain a part of it while rendering the above integral totally tractable. So, let $r^2\omega^2 \cong r^2\omega^2 \cos^2\alpha$, then:

$$D = \frac{\pi}{5} \rho a^2 \int_{\delta}^{\varphi_0} 2 \int_0^{\frac{\pi}{2}} (V + a\omega \cos\varphi) \cdot V \sin^3\varphi \cdot \cos^2\psi \cdot d\varphi d\psi \quad (19)$$

Thus:

$$D = \frac{\pi^2 \rho a^2 V^2}{240} [F_1(\varphi_0) - F_1(\delta)] \quad (20)$$

where:

$$F_1(\varphi) = 8\cos^3\varphi - 24\cos\varphi + \frac{6a\omega}{V} \sin^4\varphi \quad (21)$$

Following the same procedure, the lift, L , acting upwards along the y - axis, is given by:

$$L = \int_S^{\varphi_0} dF_n \cdot \cos\varphi \quad (22)$$

or:

$$L = \frac{\pi}{5} \rho a^2 \int_{\delta}^{\varphi_0} 2 \int_0^{\frac{\pi}{2}} \sqrt{V^2 + 2r\omega V \cos\alpha + r^2\omega^2} \cdot V \sin^2\varphi \cdot \cos\psi \cdot \cos\varphi d\varphi d\psi \quad (23)$$

Finally:

$$L = \frac{\pi\rho a^2 V^2}{240} [F_2(\varphi_0) - F_2(\delta)] \quad (24)$$

where:

$$F_2(\varphi) = 32\sin^3\varphi + \frac{3a\omega}{V} (4\varphi - \sin 4\varphi) \quad (25)$$

The two components of the hydrodynamic force are used in the equations of motion of the sphere to calculate the horizontal and vertical displacements and velocities of the sphere whereby the trajectory of the sphere can be determined.

Hence:

$$m \frac{dV_x}{dt} = -F_x = -(D \cdot \cos\lambda - L \cdot \sin\lambda) \quad (26)$$

Using Equations. (20 and 24):

$$\frac{4}{3} \pi a^3 \rho_s \frac{dV_x}{dt} = -\frac{\pi a^2 V^2}{240} \rho [\pi \cos\lambda \{F_1(\varphi_0) - F_1(\delta)\} - \sin\lambda \{F_2(\varphi_0) - F_2(\delta)\}] \quad (27)$$

$$\frac{dV_x}{dt} = -\frac{V^2}{320a\sigma} [\pi \cos\lambda \{F_1(\varphi_0) - F_1(\delta)\} - \sin\lambda \{F_2(\varphi_0) - F_2(\delta)\}] \quad (28)$$

Moreover:

$$m \frac{dV_y}{dt} = mg - F_y = mg - (D \cdot \sin\lambda + L \cdot \cos\lambda) \quad (29)$$

Thus:

$$\frac{4}{3} \pi a^3 \rho_s \frac{dV_y}{dt} = mg - \frac{\pi\rho a^2 V^2}{240} [\pi \sin\lambda \{F_1(\varphi_0) - F_1(\delta)\} + \cos\lambda \{F_2(\varphi_0) - F_2(\delta)\}] \quad (30)$$

or:

$$\frac{dV_y}{dt} = g - \frac{V^2}{320a\sigma} [\pi \sin\lambda \{F_1(\varphi_0) - F_1(\delta)\} + \cos\lambda \{F_2(\varphi_0) - F_2(\delta)\}] \quad (31)$$

It should be noted that:

$$\tan\lambda = \frac{V_y}{V_x} = \frac{dy/dt}{dx/dt} = \frac{dy}{dx} \quad (32)$$

$$V^2 = V_x^2 + V_y^2 \quad (33)$$

Equations (28) and (31) were solved using MATLAB, with the following initial conditions: At $t=0$, $x=y=0$, $V_x = V_0 \cos\theta_0$, $V_y = V_0 \sin\theta_0$. A flowchart of the MATLAB code is given in Fig. 5.

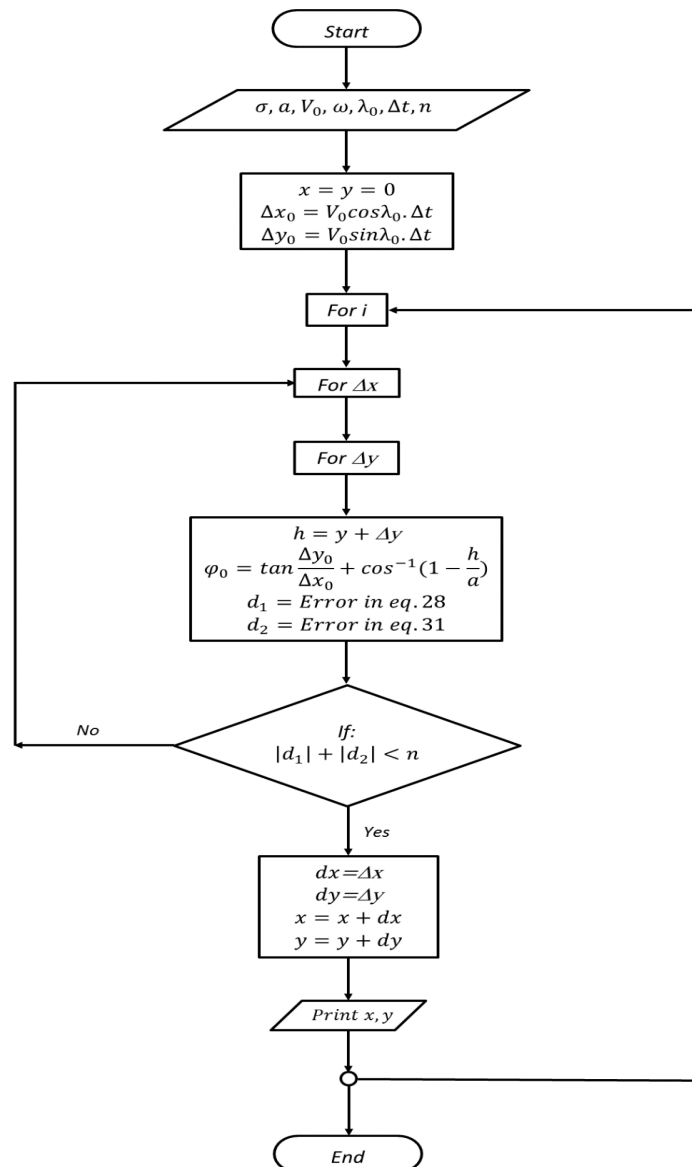


Fig. 5: MATLAB code flowchart.

3. NUMERICAL MODEL

In order to be able to judge the accuracy of the present analysis, extensive experimentations are usually recommended. However, due to the vast difficulties encountered during a single experiment, the simulation of the problem would be far more suitable in this respect. The effects of cavitation, splash, and two phase flow are negligible compared to the hydro-dynamic forces of lift and drag. ABAQUS 17-1 version was utilized to model the oblique entry of a solid sphere into water with both rotational and translational velocities. As shown in Fig. 6, the model consists of two entities, namely "water box" and "Aluminum sphere". The water box dimensions are 600, 120, and 70 mm and the radius of the ball is invariably 10 mm. The length of the water box was chosen such that the sphere has enough water space during the expected course of travel of the sphere. Other sides of the water box were selected as non-reflecting edges to neglect the effect of reflecting waves. The initial translational velocity is fixed at 10 m/sec while the rotational speeds considered are 0, 100, 200, and 300 rad/sec.

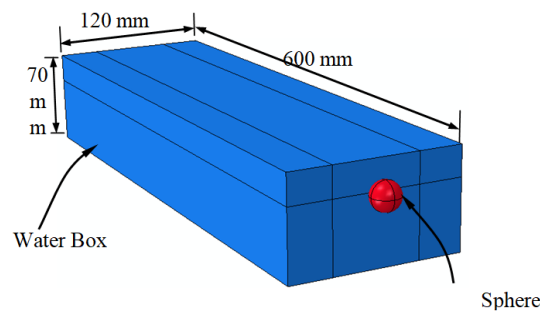


Fig. 6: Schematic drawing of the assembled model.

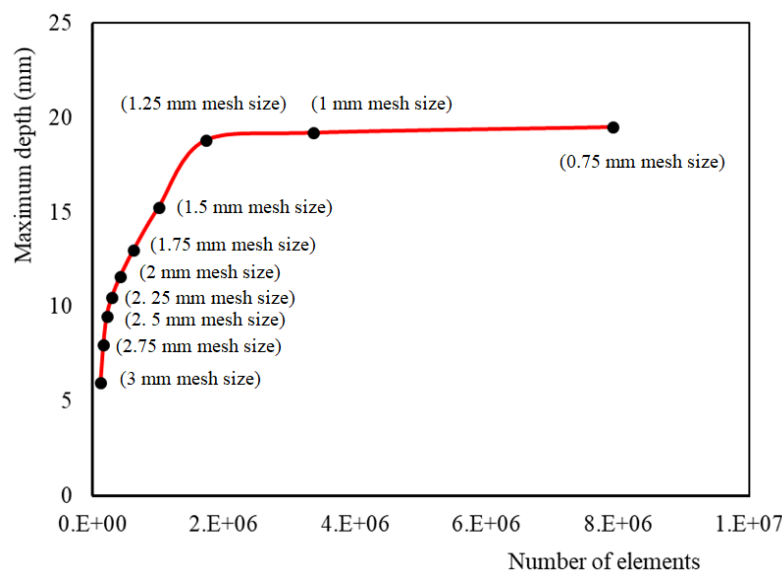


Fig. 7: Mesh convergence, $\lambda_0=11$ deg.

Referring to Fig. 7, the maximum depth was selected according to the mesh size. It remained almost stable beyond the 1.25 mm mesh size (1720320 elements). For reasonably accurate results with possible run times, the 1.25 mm element size was selected. The type selected for mesh elements of the water box was EC3D8R (An 8-node linear Eulerian brick, reduced integration, hourglass control), while C3D10M (A 10-node modified quadratic tetrahedron) was assigned for the aluminum ball. This model was capable of capturing the effect of the attack angle of the aluminum sphere upon ricochet against the water surface.

4. RESULTS AND DISCUSSION

The oblique entry of aluminum ($\sigma = 2.7$) spinning spheres of radius 10 mm and speed of 10 m/sec ($Fr = 32$) was determined analytically and simulated as well. As a benchmark, the non-spinning case was also considered.

The present analysis proposes two differential equations of motion of the sphere, Equations (28) and (31), in x- and y- directions respectively. An algorithm was built to solve these equations for different values of angle between the sphere flight and the water surface. Critical angles of ricochet were sought for a non-spinning sphere as well as for spheres spinning at 100, 200, and 300 rad/sec, as shown in Figs. 8, 9, 10 and 11, respectively.

In these figures, positions of the sphere were determined from the moment of initial contact with water (at origin of graph) to the moment of either total emergence from the water (i.e. ricochet) or eventual sinking. According to the definition of the limiting condition of ricochet, the whole sphere emerges with just a horizontal speed. This implies that the trajectory of the sphere in this case has a local maximum point located right on the water surface. As seen in Figs. 8(A), 9(A), 10(A) and 11(A) the trajectories of ricocheting spheres almost exhibit local maxima at the water surface; exact determination of these maxima was dictated by effort and time of computation. On the other hand, a non-spinning sphere eventually sinks (or non-ricochet) if it is fully submerged, see Fig. 8(B). This, of course, is attributed to the fact that the sphere in this case has no more hydrodynamic lift to overcome the gravity. Another explanation is also provided by Equations (24) and (25) for $\omega=0$ and $\varphi_0 = \pi$. Since the spinning spheres are continually experiencing lift, even when they are totally submerged, the sphere is said to be in a state of non-ricochet only if it reaches the local maximum point without total emergence from the water surface, see Figures 9(B), 10(B) and 11(B).

Compared with the experimental findings of Richardson [2], the trajectories of ricochet in Figs. 8-11(A) resemble that depicted in Fig. 1(b), while those of non-ricochet resemble that of Fig. 1(c).

Of special interest is the uniform motion of the sphere at the end of its course of entry, see Fig.9(B). This suggests that the lift is just counteracted by gravity by the time the drag ceases to exist.

The values of the critical angle of ricochet and non-dimensional maximum depth of submergence at critical ricochet, for non-spinning sphere drawn from the above mentioned figures, are listed in Table 1 together with available published data.

Table 1: Comparison of the critical angle of ricochet λ_c and the non-dimensional maximum depth of submergence at critical ricochet, y_{max}/a for non-spinning sphere with published data.

Ref.	Present work	Exp.[2]	Eq.(1).[3]	Eq.(2).[4]	Eq.(4).[5]	Analytic [7]
λ_c , deg.	10.43	9	10.95	10.65	10.53	10
y_{max}/a	1.56	-----	-----	2.00	1.00	1.16

Except for $\lambda_c = 90$, the present analysis prediction is favorably in agreement with the available data. The experimental value reported by Richardson [2], $\lambda_c = 90$, was previously discussed by Johnson & Reid [4] who attributed this variation to the extremely low Froude number.

The non-dimensional maximum depth of submergence at critical ricochet, y_{max}/a , is determined from the trajectory of the sphere. As apparently seen in Table 1, the present analysis falls within the previously assumed values in References [4,5] and the numerically computed value in Ref. [7]. In the absence of extensive experimental work, the discrepancies shown in Table 1 cannot be presently resolved.

A similar presentation of results was addressed to the effect of spin in order to assess the desired benefits, if any, when a back spin is imparted to a solid sphere entering the water. Table 2 is a summary of the results drawn from Figs. 9, 10, and 11.

Table 2: Analytical values of critical ricochet angle and max. immersion depth.

Backspin, ω (rad/s)	0	100	200	300
Critical ricochet angle, λ_c (deg.)	10.43	11.1	11.7	12.5
Max. immersion depth, y_{max}/a	1.56	1.64	1.74	1.86

It is clear that the backspin enhances the tendency of the sphere towards ricocheting off the water surface and that the enhancement is higher at higher values of spin. Moreover, the sphere experiences higher depths of submergence at higher values of spin. No relevant previous works are available with which a comparison of these findings could be made, since the effect of spin, on the characteristics of sphere impact with water, is only presently investigated.

Data from Figs. 8 through 11 were rearranged to display the influence of spin on the range of contact of the sphere with water for the cases of critical angles of ricochet, as displayed in Fig. 12. It is obvious that the increase in maximum depth of immersion due to spin is accompanied by a shortening in the range of contact, and the effect is nonlinear. This can be returned to the direct proportionality of the lift force with the spin.

"Magnus effect", widely known in spinning solids of revolution in air, is especially addressed in this work. For this purpose, the experimental finding of Truscot & Techet [10], shown in Fig. 2(b), was chosen. In this experiment, a ball enters the water pool normally with translational as well as rotational speeds. The same data of the experiment were used in the present analysis, whereby the trajectory of the spinning sphere was computed and plotted as shown in Fig. 13. The comparison is merely qualitative in that the present analysis is capable of predicting the evident curvature in the path of sphere motion which manifests considerable lift forces induced by spin. Nevertheless, the comparison is reasonable in terms of vertical and lateral displacements of the sphere. The drag and lift forces acting on a submerged sphere can be estimated by means of Equations (20), (21), (24) and (25) in conjunction with $\varphi_0 = \pi$ and $\delta = 0$. Hence:

$$D = \frac{\pi\rho a^2 V^2}{12} \quad (34)$$

$$L = \frac{\pi\rho a^3 \omega V}{16} \quad (35)$$

Numerical analysis was presently performed using ABAQUS 17-1 version to simulate the process of oblique impact of spheres with the water surface. A typical example of the simulation of the ricochet process is displayed in Fig. 14. The critical angle of ricochet for the same four cases, namely non spin and 100, 200, and 300 rad/s-spins, were sought. The trajectories for these critical cases are gathered as shown in Fig. 15. Similar trends to those found analytically in Fig. 12, were observed. This suggests that the ricochet process can well be simulated and used in extensive studies of similar processes. The process of simulation is highly sensitive to the mesh size and hence the number of elements. The optimum size was governed by the conditions prevailing in such an event on one hand and in the other hand by the inevitable limitations of time and effort. In Fig. 15, the range of sphere trip of ricochet differs slightly from the analytical results of Fig. 12, in value as well as in the nature of dependence with spin. The difference, however, lies within the range of scatter cited in the available data. The critical angle of ricochet as well as the non-dimensional maximum depth of immersion were extracted from the trajectories and listed in Table 3. For purpose of

comparison between the analytical and numerical findings, Table 4 is constructed by collecting the data of Tables 3 and 4.

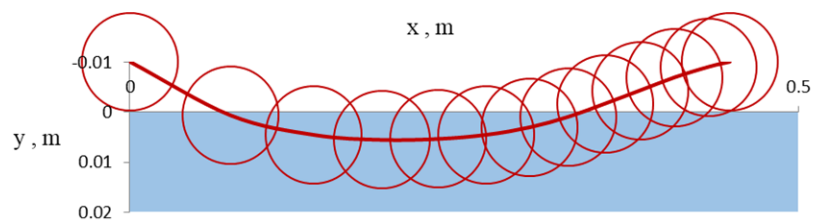
Table 3: Numerical values of critical ricochet angle and max. immersion depth

Backspin, ω (rad/s)	0	100	200	300
Critical ricochet angle, λ_c (deg.)	10.75	11.35	12	12.8
Max. immersion depth, y_{max}/a	1.52	1.62	1.71	1.83

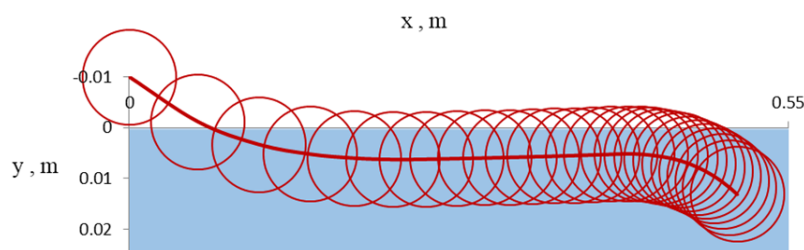
Table 4: Analytical and numerical values of critical ricochet angle and max. immersion depth

Backspin, ω (rad/s)	Critical ricochet angle, λ_c (deg.)		Max. immersion depth, y_{max}/a	
	Analytical	Numerical	Analytical	Numerical
0	10.43	10.75	1.56	1.52
100	11.1	11.35	1.64	1.62
200	11.7	12	1.74	1.71
300	12.5	12.8	1.86	1.83

As revealed by Table 4, the simulation results in higher values for the critical angle of ricochet than that found by the analysis. On the contrary, the simulation predicts lower values regarding the maximum depth of immersion. This suggests that the hydrodynamic forces in the simulation were higher than those assumed in the analysis. The variation in analytical with numerical results can be reduced either by increasing the constant ($\pi/5$) in the pressure formula, Eq. (7), or selecting moderate pressures in the simulation process. Either way is only possible or favorable in the presence of extensive experimentation as the actual and realistic datum.



(a) Ricochet, $\lambda_0 = 10.43 \text{ deg}$



(b) Non ricochet, $\lambda_0 = 10.45 \text{ deg}$

Fig. 8: Trajectories of non-spinning sphere at different angles of attack.

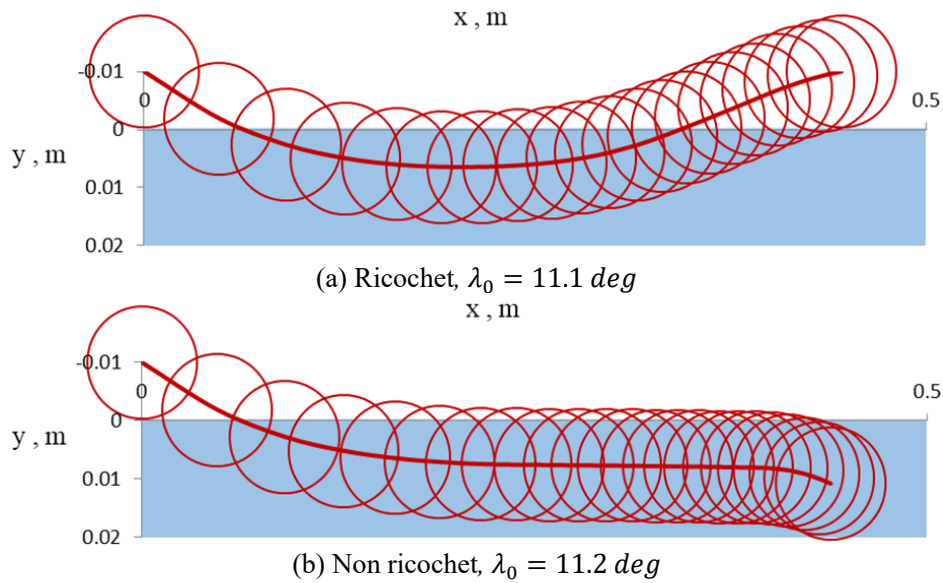


Fig. 9: Trajectories of sphere spinning at $\omega=100$ rad/sec at critical angles of attack.

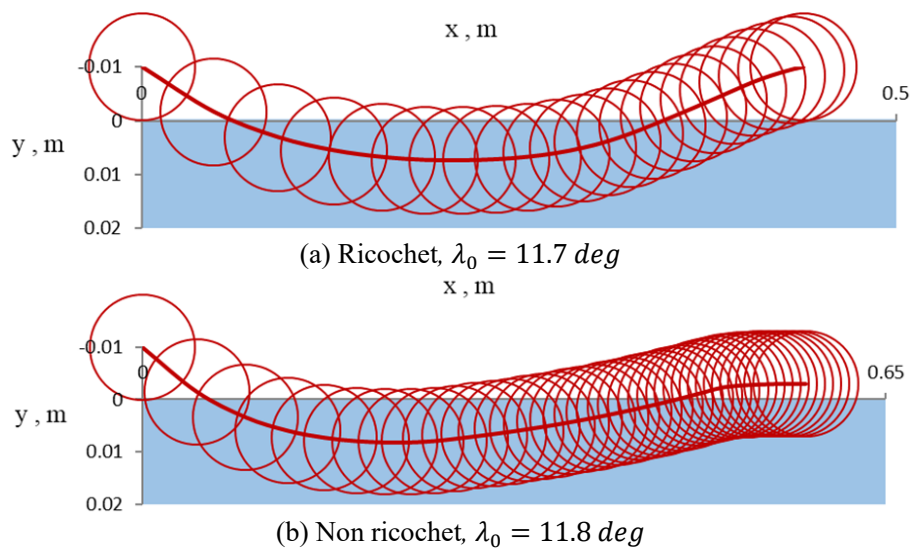
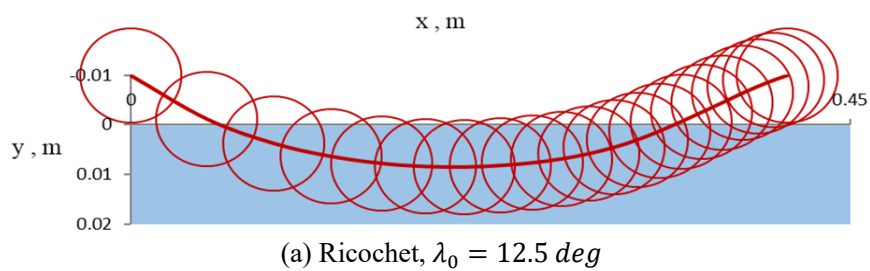


Fig. 10: Trajectories of sphere spinning at $\omega=200$ rad/sec at critical angles of attack.



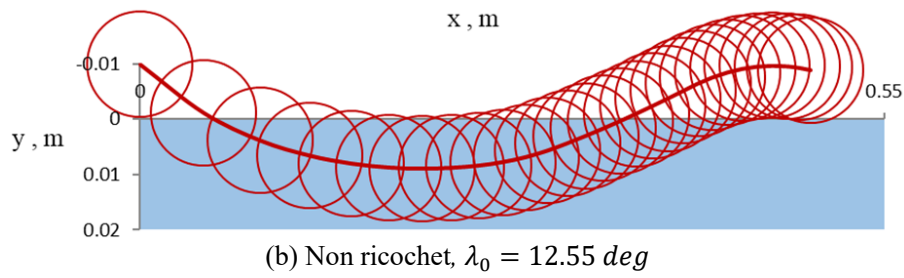


Fig. 11: Trajectories of sphere spinning at $\omega=300$ rad/sec at critical angles of attack.

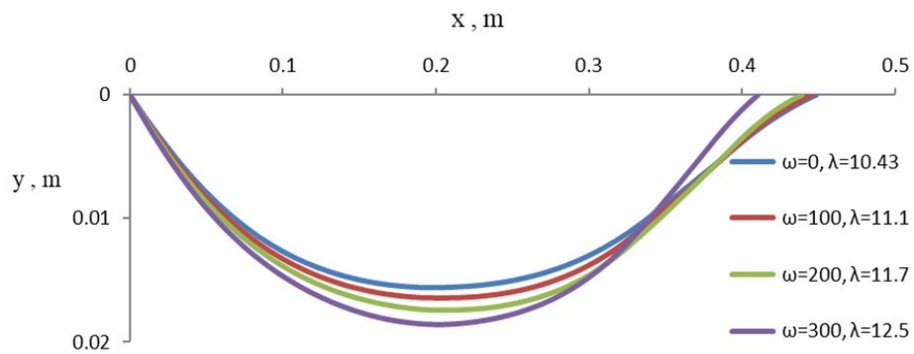


Fig. 12: Analytical trajectories of ricocheting sphere spinning at different values of spin and critical angles of attack.

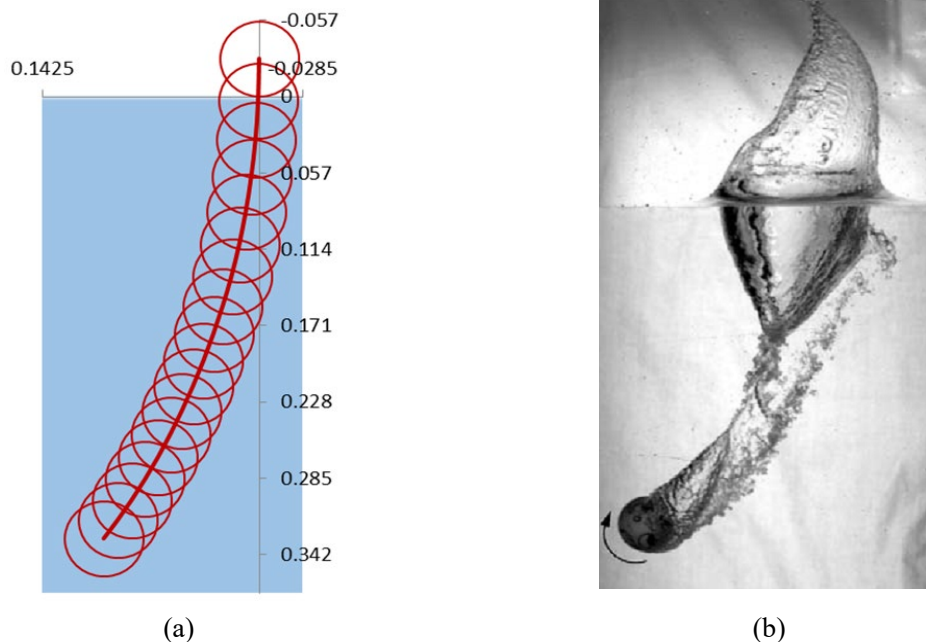


Fig. 13: Qualitative comparison between the trajectories of spinning spheres:
(a) Present analysis, (b) Experiment [10].

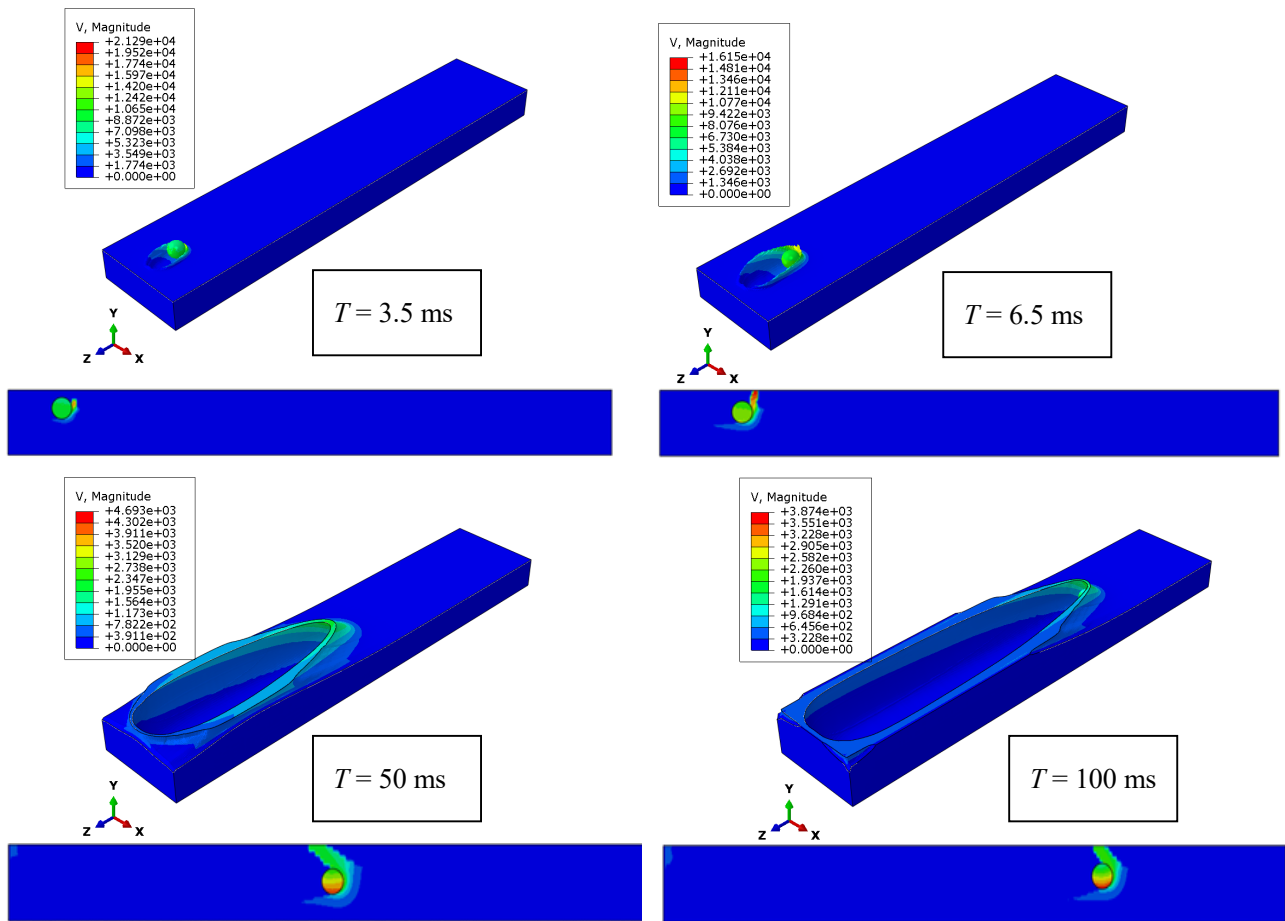


Fig. 14: Simulation of the ricochet process.

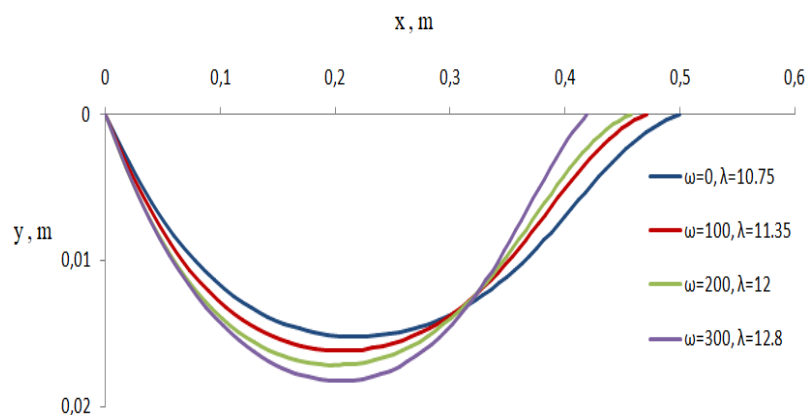


Fig. 15: Numerical trajectories of ricocheting sphere spinning at different values of spin and critical angles of attack.

5. CONCLUSIONS

Liquid-solid interaction phenomena are still receiving the attention of engineers and scholars in view of the rapid advances in technology. The research in the field of ricochet of solid spheres from water surfaces, though seemingly exhausted, is yet far from being well established. A consensus now exists related to the tendency of a sphere to ricochet from

water, i.e. ricochet is more likely with high translational and backspin speeds, low density, large diameter, and low angle of impact.

Although the process is highly complex and no single work can handle all the parameters and their effects, the present work assumes that the effects of cavitation, splash, and two phase flow are negligible compared to hydro-dynamical forces of lift and drag. The main contributing conclusions are:

1. A theoretical analysis, based on a previous one and modified for the spin, is made.
2. The maximum critical angle of ricochet increases with backspin of the sphere. A backspin of 300 rad/sec improves the angle from 10.43° to 12.5° .
3. The non-dimensional maximum depth also increases with backspin. A backspin of 300 rad/sec increases the depth from 1.56 to 1.86.
4. The theoretical analysis was found capable of describing previous experimental work, as well as matching other analytical and numerical works.
5. A numerical model simulation of fluid-structure and ricochet of spinning spheres was also made using ABAQUS 17-1 version.
6. The implementation of ABAQUS was efficient in simulating the ricochet process.
7. The analytical and numerical results were consistent in that the backspin enhances the capability of a sphere in performing ricochet.
8. Magnus effect in liquids was presently described and relations predicting the drag and lift forces were deduced.
9. The analytical and numerical results vary to the same extent of variation of hydrodynamic forces.
10. A detailed and extensive experimental work is highly recommended to end the widely cited debate among other works.

REFERENCES

- [1] Johnson W. (1997) The ricochet of spinning and non-spinning spherical projectiles, mainly from water. Part II: An outline of theory and warlike applications. *Int. J. Impact Engineering*, 21: 25-34. [https://doi.org/10.1016/S0734-743X\(97\)00033-X](https://doi.org/10.1016/S0734-743X(97)00033-X).
- [2] Richardson EG. (1948) The impact of a solid on a liquid surface. *Proc. Phy. Soc.*, 61: 352-367. <https://doi.org/10.1088/0959-5309/61/4/308>.
- [3] Birkhoff G, Birkhoff GD, Bleick WE, Handler EH, Murnaghan FD, Smith TL. (1944) Ricochet off water. *App.Math. Panel, National Defense Research committee, Memo. 42, 4M, AMG-C*.
- [4] Johnson W, Reid SR. (1975) Ricochet of spheres off water. *J. Mech. Engineering. Sci.*, 17: 71-81. https://doi.org/10.1243/JMES_JOUR_1975_017_013.
- [5] Hutchings IA. (1976) The ricochet of spheres and cylinders from the surface of water. *Int. J. Mech. Sci.*, 18: 243-247. [https://doi.org/10.1016/0020-7403\(76\)90006-0](https://doi.org/10.1016/0020-7403(76)90006-0).
- [6] Soliman AS, Reid SR, Johnson W. (1976) The effect of spherical projectiles speed in ricochet off water and sand. *Int. J. Mech. Sci.*, 18: 279-284. [https://doi.org/10.1016/0020-7403\(76\)90029-1](https://doi.org/10.1016/0020-7403(76)90029-1).
- [7] Miloh T, Shukron Y. (1991) Ricochet off water of spherical projectiles. *J. Ship Research*, 35: 91-100. <https://doi.org/10.5957/jsr.1991.35.2.91>.
- [8] Park MS, Jung YR, Park WG. (2003) Numerical study of impact force and ricochet behavior of high speed water-entry bodies. *Computers & Fluids*, 32: 939-951. [https://doi.org/10.1016/S0045-7930\(02\)00087-7](https://doi.org/10.1016/S0045-7930(02)00087-7).

- [9] Rosellini L, Hersen F, Clanet C, Bocquet L. (2005) Skipping stones. *J. Fluid Mech*, 543: 137-146. <https://doi.org/10.1017/S0022112005006373>.
- [10] Truscott TT, Techet AH. (2009) Water entry of spinning spheres. *J. Fluid Mech.* , 625: 1-31. <https://doi.org/10.1017/S0022112008005533>.
- [11] Wei Z, Shi X , Wang Y. (2012) The oblique water entry impact of a torpedo and its ballistic trajectory simulation. *Int. J. Numerical Analysis and Modeling*, 9: 312–325. https://doi.org/10.1007/978-3-642-11842-5_62.
- [12] Moxnes JF, Frøyland Ø, Skriudalen S, Prytz AK, Teland JA, Friis E. (2016) On the study of ricochet and penetration in sand, water and gelatin by spheres, 7.62 mm APM2, and 25 mm projectiles. *Defence Technology*, 12: 159-70. <https://doi.org/10.1016/j.dt.2015.12.004>.
- [13] Omidvar P, Farghadani O, Nikeghbali P. (2017) SPH for impact force and ricochet behavior of water-entry bodies. *Int. J. Modern Physics C.*, 28: 1750119. <https://doi.org/10.1142/S0129183117501194>.
- [14] Nguyen VT, Phan TH, Park WG. (2020) Modeling and numerical simulation of ricochet and penetration of water entry bodies using an efficient free surface model. *Int. J. Mech. Sci.*, 182: 105726. <https://doi.org/10.1016/j.ijmecsci.2020.105726>.
- [15] Nguyen VT, Phan TH, Duy TN , Park WG. (2021) 3D simulation of water entry of an oblique cylinder with six-degree-of-freedom motions using an efficient free surface flow model. *Ocean Engineering*, 220: 108409. <https://doi.org/10.1016/j.oceaneng.2020.108409>.
- [16] Lyu X , Yun H, Wei Z (2021) Experimental Study of a Sphere Bouncing on the Water. *Journal of Marine Science and Application*, 20: 714-722. <https://doi.org/10.1007/s11804-021-00236-9>.

Nomenclature			
a	Radius of sphere	x, y, z	Coordinate axes
D	Drag force	ω	Angular velocity of sphere
F_n	Hydrodynamic force normal to solid surface	σ	Specific density of sphere
F_x	Horizontal component of hydrodynamic force	β	Angle of obliquity of plane relative to liquid flow
F_y	Vertical component of hydrodynamic force	ρ, ρ_s	Density of liquid and sphere
\bar{F}	Froude number = \bar{V}/\sqrt{ag}	θ	Angle of rotation
L	Lift force	ϑ_c	Critical angle of ricochet
m	Mass of solid	φ	Longitude angle
n	Error allowance	Ψ	Latitude angle
p	Hydrodynamic pressure of liquid	λ	Current angle of travel of sphere
r	Radius of rotation	λ_0	Initial angle of travel of sphere
S	Area of sphere surface	φ_0	Angular extent of wetted area
V', V	Velocity of liquid flow relative to sphere surface	θ_0	Angle of entry
V_0	Speed of entry	Δt	Time interval